ORIGINAL PAPER

# Preparation and characterization of carboxylated styrene butadiene rubber (XSBR)/multiwall carbon nanotubes (MWCNTs) nanocomposites

**Mohammad Alimardani · Foroud Abbassi-Sourki · Gholam Reza Bakhshandeh**

**Abstract** This study deals with the preparation of carboxylated styrene butadiene rubber (XSBR)/multiwall carbon nanotubes (MWCNTs) nanocomposites prepared in the latex form by means of a ball mill. Two types of CNTs, i.e., non-functionalized and OH-functionalized (CNT–OH) were used. The rheological properties, FTIR spectrums, SEM micrographs and stress relaxation experiments were exploited to evaluate the resulting nanocomposites. For a given frequency, both the viscosity and storage modulus increased as the concentration of CNT was augmented with the greatest value for the nanocomposites loaded with CNT–OH. The viscosity of nanocomposites exhibited a shear thinning behavior throughout applied frequency and indicated a power law index of about $n = 0.22$. Nanocomposite ATR analyses revealed the presence of physical interaction of H-bonding type between hydroxyl group of CNT–OH and carboxyl group of XSBR for XSBR–CNTOH nanocomposites. A mechanism based on the chemistry of medium was proposed to explain the development of H-bonding. SEM micrographs confirmed the uniformity of carbon nanotubes dispersion in the resulting microstructure. A two-step innovative stress relaxation experiment was performed on the prepared nanocomposites through which the resulting microstructure of nanocomposites was further explored. The relaxation behavior of nanocomposites (both in first and second steps) were modeled and well predicted using Prony series and the parameters of generalized Maxwell equation for stress relaxation, $\tau_i$ and $g_i$ were computed, as well.

## Introduction

Polymer nanocomposites are a progressively large category of hybrid materials. Since the introduction of carbon nanotubes (CNTs), their nanocomposites have attracted an immense attention [1, 2]. Due to the unique optical, electrical, rheological and mechanical properties they are introduced to the polymer matrix. However, even after two decades of research, the use of CNTs as an established reinforcing agent has been extremely limited. The arising restrictions are mainly due to difficulties associated with the dispersion and breakup of the bundles of CNT self-assembles during processing and the poor interfacial interaction between CNT and macromolecular chains of polymer matrix.

As a result of strong van der Walls forces resulting from high specific surface area and small size, CNTs have tendency to agglomerate and form clusters which are hard to be broken by normal mixing apparatus. In fact, the key challenge is to obtain a homogeneous dispersion of CNT in the matrix. To do so and to exploit the exclusive advantages of this material, the aggregates should be broken. The eventual result in the enhancement of the interfacial bonding leads to prevent slippage. The assessment of CNT dispersion is another obstacle of this field.

Due to the nano size dimension, optical microscopy methods cannot be helpful to characterize these materials. Electronic microscopes are frequently used for this issue; however, they show just a scant part of a sample rather than the whole bulk. Hence, the results could be deceptive.

M. Alimardani · F. Abbassi-Sourki (✉) · G. R. Bakhshandeh
Department of Polymer Processing, Iran Polymer and
Petrochemical Institute, P.O. Box: 14965/115, Tehran, Iran
e-mail: F.Abbasi@ippi.ac.ir

Fortunately, CNT composites present obvious differences in the electrical, viscoelastic and rheological properties compared with virgin polymers that can be taken into account as a reliable measure to confirm the microscopic results.

Rheological properties of CNT/polymer nanocomposites depend upon numerous parameters such as filler characteristics, filler loading, aspect ratio, state of dispersion of filler, polymer molecular weight, and interfacial interaction between the polymer and filler. Having eliminated the effects of CNT loading, its aspect ratio, and polymer molecular weight, changes in rheological properties can be attributed to the state of dispersion of CNT and quantity and quality of its interfacial interactions with polymer.

Studies indicate that the aforesaid techniques can be used to pursue the microstructure properties of nanocomposites. Huang et al. [1] investigated the dispersion rheology of CNTs in PDMS (polydimethylsiloxane) and rheologically measured the optimum time of mixing process for obtaining a good dispersion of CNT. They also investigated the influence of CNT concentration on the rheological properties of nanocomposites. Ivanov et al. [2], Via et al. [3], Yan et al. [4], Cheng et al. [5], Kim et al. [6], Rahmatpour et al. [7], and Pötschke et al. [8] examined the capabilities of rheological methods to follow the microstructure.

Carboxylated styrene butadiene rubber latex (XSBR) is a kind of high polymer dispersions prepared by emulsion polymerization of butadiene, styrene and one or more unsaturated acids such as acrylic acid, methacrylic acid, crotonic acid, maleic acid, etc. The chemical structure of XSBR is presented in Scheme 1.

Contrary to SBR latex which commonly presents slight affinity towards various nano additives, presence of carboxyl groups in the structure of its carboxylated counterpart creates active sites displaying high affinity and interaction to the most of nano additives, with either functionality or non-functionality. These interactions affect on both the dispersion process of nano additive and the viscoelastic and rheological properties of the polymer. Du et al. [9] have studied the nanocomposites of halloysite nanotube and XSBR. Their results showed that the chemical interaction between functional groups in nanotube and latex can be very effective in improving the dispersion process. Peterson et al. [10], Pietrasik et al. [11], Jubete
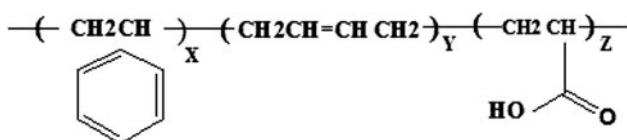
et al. [12] and Stephen et al. [13]. have carried out similar tasks on the use of carboxyl group in rubber latices to increase the interfacial interaction of materials in composites.

This article is the first part of a comprehensive study concerning CNT/XSBR composites carried out in our laboratory. Despite the practical importance of latex composites, CNT/XSBR composites have received no or less attention, and to the best of our knowledge, there is a lack of rheological and viscoelastic investigations concerning these materials. In the first part, subsequent to preparing CNT/XSBR nanocomposites, rheological examinations and simple stress relaxation experiments were performed on the prepared samples to characterize the microstructure of composites. In the second part, a combined two-step strain stress relaxation was used to further investigate the effect of CNT on the microstructure of resulting nanocomposites. Infrared spectra and SEM micrographs of the samples were used to explain and endorse the obtained results. Eventually, relaxation behaviors of nanocomposites were modeled by Prony series and then, the parameters of generalized Maxwell stress relaxation equation, $\tau_i$ and $g_i$, were computed.

## Experimental

### Materials

Carboxylated styrene butadiene copolymer (XSBR), M 100 grade, with 50 wt % solid contents and 0 °C glass transition temperature was supplied by Paya Rezine Company, Iran. Functional and non-functional multiwall carbon nanotubes characterized by a length of 10–20 μm and a diameter of 20 nm were purchased from Neutrino Co., Iran. The functionalized CNT was hydroxyl type, abounding in 4 %. SDS (sodium dodocyle sulfate) surfactant was purchased from Aldrich.

To prepare a nanocomposite, first SDS surfactant was dissolved in distilled water and then, multiwall carbon nanotubes (MWCNT) was added to the solution. The weight ratio of carbon nanotube to the surfactant was always kept at 1/3. The resulting solution was then added to the XSBR latex. The samples were ball milled for an optimized time of 6 h and then dried at the temperature of 40 °C in an oven for 48 h. Since the aim was to study the microstructure of XSBR/nanotube nanocomposite, the samples were prepared free of any extra ingredients generally added for the various purposes. In order to use small quantity of carbon nanotube, we fabricated a small home-made ball mill using a stainless steel container with a diameter and height of 8 and 12 cm, respectively, and 400 small stainless steel balls in two different sizes of 0.6

Scheme 1 Chemical structure of carboxylated styrene butadiene rubber

and 0.8 mm. Based on a fundamental operative relationship describing the optimum speed of milling, a rate of 60 rpm has been chosen for a vessel of this size [14].

### Instruments

Rheological properties and stress relaxation experiments were carried out on a rubber process analyzer (RPA2000, Alpha Technologies, USA). The instrument is capable of imposing any desired strain, frequency and temperature. For frequency sweep tests, a temperature of 90 °C and a strain of 5 % were applied. Details of relaxation experiment will be given later. FTIR analyses were carried out on an Equinox 55 (Bruker, Germany) instrument in ATR mode and at the wave number range of 600–4,000 cm$^{-1}$ and finally SEM micrographs were prepared at the magnification of 15,000×, 45,000× and 54,000× using a WEGA\TESCAN electron microscope (JSM-5800 of JEOL Co., Japan); acceleration voltage: 20 kV; type of coating: gold.

## Results and discussion

### Rheological measurements

Various techniques such as ultrasonication, calendaring, extrusion and ball milling are applied to disperse carbon nanotubes in polymer matrices. Ball milling is a highly effective means to introduce a second phase, solid or liquid, to a liquid matrix phase. Experimental investigations show that an excellent dispersion of poor dispersing material can be achieved using this method [14]. In addition ball mills are widely applied for the same purpose at larger scales and industrial plants which makes the scale up of a laboratory to be rather easy.

Ball milling has been appropriately used to disperse CNTs for different purposes, for example, to modify the microstructure of cup-stacked CNTs, to produce different carbon nanoparticles from graphitic carbon for hydrogen storage applications and to transform CNTs into nanoparticles [15–17]. Ball milling of CNTs with solid or liquid can enhance breakup the entanglements, therefore it would increase the dispersion of CNTs in polymer matrix [18]. On the other hand, both ball mill and ultrasonication methods are a little destructive to CNTs. To minimize such adverse effects, various parameters which can affect the efficiency of milling should be adjusted according to available standards and data. The important factors are milling time, milling speed, size of balls, size distribution of balls, volume of balls and the slurry charged, mill diameter and the viscosity of slurry.

Milling time strongly affects the mechanical properties and the microstructure of composites [18] therefore in the
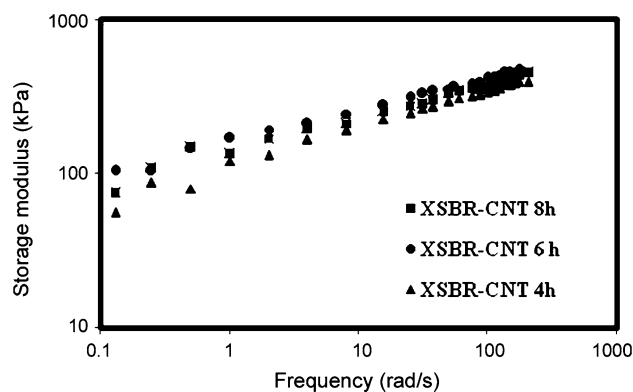


**Fig. 1** Variations of storage modulus as a function of frequency for various ball milling durations

first step, optimization of operating time seems essential. Thus, three samples of XSBR/MWCNTs nanocomposites were prepared. Minimum milling time was adjusted at 4 h for the first batch followed by 6 and 8 h for other two batches. All other parameters were similar.

Figure 1 represents the storage modulus (G′) as a measure of dispersion (later will further be discussed) of the aforesaid samples plotted against frequency. All three samples show an increase in G′ as frequency approaches higher values. As the milling time went beyond 4 h, the storage modulus increased, however, a longer time of milling (8 h) leaded to an adverse effect and decreased the modulus of the resulting sample. As mentioned earlier, ball milling is a little destructive to some fibrous additives, particularly when the milling duration is extended to longer time. Hence, applying 8 h milling resulted in further breakup of CNTs to shorter particles which resulted in weaker rheological properties. In other words, milling for 6 h was quite sufficient to provide a good dispersion with minimum negative effects of milling.

To guarantee the reproducibility of the results and the accuracy of milling equipment, the process was repeated for another 6 and 8 h on new samples. The results were almost identical from both qualitative and quantitative points of view, as shown in Fig. 2. Since the all other parameters in preparation procedure and milling process were similar, the observed improvement in rheological properties can be attributed to the morphology of CNT in polymer matrix.

Incorporation of any filler to a polymer matrix leads to a change of both rheological and viscoelastic properties which may be used as a promising means to evaluate the changes resulting from the presence of CNT in rubbers. Figures 3, 4 demonstrate the complex viscosity and storage modulus versus frequency of various XSBR/CNT samples at 5 % fixed strain and 90 °C, respectively. The concentration of CNT (non-functionalized) varied as 0 (pure XSBR), 1, 2 and 4 phr. As the imposed frequency was
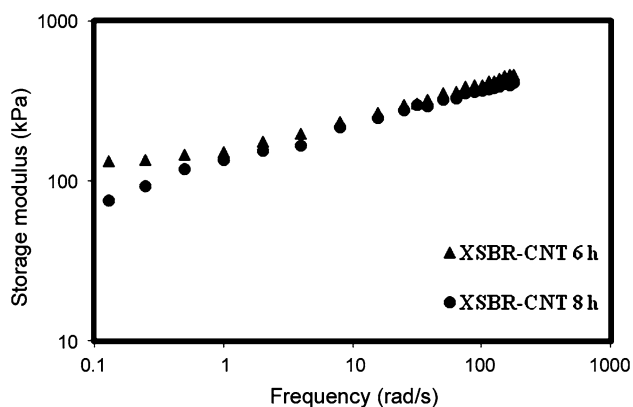
**Fig. 2** Variations of storage modulus as a function of frequency for various ball milling durations, repetition of experiments for reproducibility of results

raised, the complex viscosity decreased indicating a shear thinning behavior. This is attributed to the orientation of polymer chains and the network originating from the interaction between elastomer and nanotubes. According to Cox-Merz rule as follows [19]:

$$\eta(\dot{\gamma}) = \left| \overset{*}{\eta}(\omega) \right| \tag{1}$$

shear rate dependency of steady state viscosity is equivalent to frequency dependency of the linear complex viscosity. In this equality, $\eta$ and $\overset{*}{\eta}$ are the steady shear and complex viscosities, $\dot{\gamma}$ represents the shear rate and $\omega$ is the frequency.

Therefore, a high frequency may be accounted for a high shear rate at which the sample is subjected to high strain leading to large deformation of the compound. Applying a frequency (shear rate) to a network causes the available interactions between nanotubes and the macromolecular chains to get weak followed by the rearrangement of both macromolecules and nanotubes. The arising new morphology consists of the alignment of carbon nanotubes in
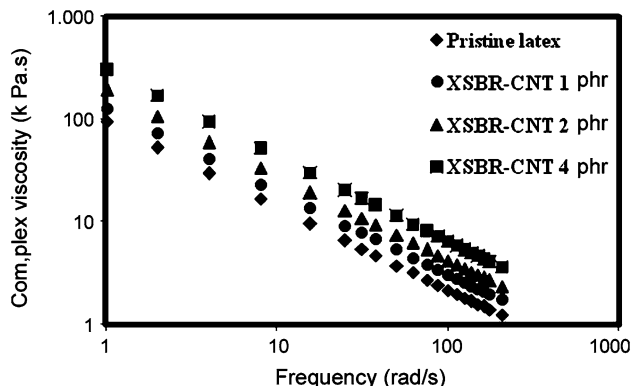
the direction of shear force, presenting less conflict with the applied strain. Very interestingly, the logarithm of complex viscosity thins linearly with logarithm of frequency and indicates a power law behavior with an index of $n = 0.2$. Despite the larger value of viscosity for the CNTs filled XSBRs, their power law indexes, $n$, varies between 0.2 and 0.24 for filled and unfilled compounds indicating a similar dependence of filled compounds on the frequency (and therefore on shear rate; Cox-Merz rule). It may be ascribed to the destruction of network developed physically between nanotube and polymer chains, as a result of applied frequency or equivalent shear.

Changes of modulus with frequency have been exhibited in Fig. 4 for non-functionalized CNT filled XSBR. As the imposed frequency approaches the natural frequency of Brownian motion, the dynamic modulus increases and finally reaches high values characterizing glassy solids. Eventually, at sufficiently high frequencies, the molecules do not move at all, rather start to vibrate at an amplitude with a small range [20, 21]. The storage modulus attains higher value as the concentration of CNTs increases indicating higher number of interactions between polymer chains and CNTs. The lowest modulus is observed for pristine latex.

The functionalized CNT filled XSBR (XSBR/CNTOHs) presents greater modulus compared to non-functionalized one (XSBR/CNTs) representing an even dispersion of CNTs and strong interaction between functional groups of polymer (carboxyl groups) and those (hydroxyl groups) of CNTs. The higher the number of bonding between macromolecules and CNT functional groups, the stronger is the polymer/CNTs network. This subject will be fully discussed in the next section.

Incorporation of functionalized CNTs into the XSBR results in a higher storage modulus at an equal CNTs concentration compared to the non-functionalized counterpart. This is exhibited in Fig. 5 where the storage
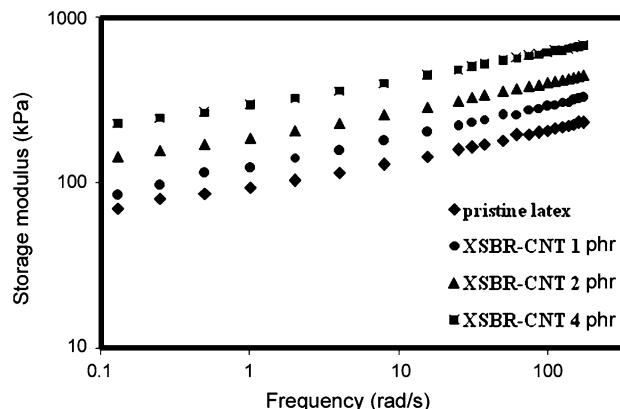


**Fig. 3** Viscosity changes as a function of frequency for nanocomposites loaded with various concentrations of CNTs



**Fig. 4** Effect of CNTs concentration on the storage modulus as a function of frequency
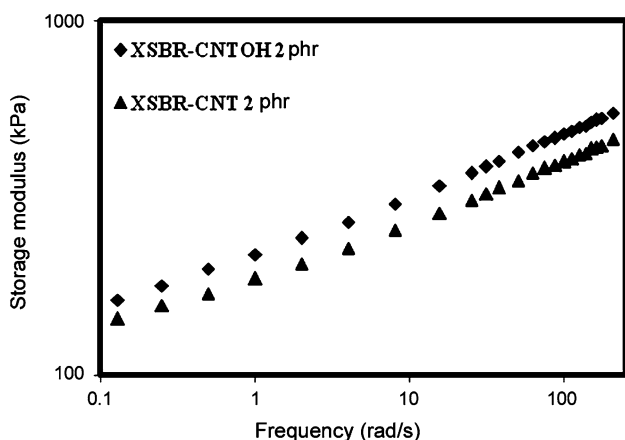
**Fig. 5** Comparison of storage moduli as a function of frequency for nanocomposites prepared by adding 2 phr functionalized and non-functionalized CNTs

modulus of nanotube filled XSBR latex was plotted against frequency. Presence of hydroxyl groups on the surface of nanotubes which makes stronger bridge between nanotubes and polymer chains is accounted for higher modulus. Furthermore, when hydroxyl functions and carboxyl groups, grafted on the polymer chain, lie in close vicinity, developed hydrogen bonds among them lead to even better dispersion of nanotubes (at molecular level) in the matrix. The eventual result is a higher elasticity of sample reinforced with 2 phr functionalized CNTs throughout the applied frequency.

As the frequency is increased, the priority of XSBR/CNTOHs sample modulus over that of XSBR/CNT becomes more pronounced. We link this superiority in modulus to the capability of latex carboxyl groups to make hydrogen bonding with hydrogen atoms of hydroxyl functional group of carbon nanotubes. In fact, Fig. 5 evidently proves the occurrence of this type of bonding and the stability of the network made by such physical link. Furthermore, hydrogen bonding plays a major role in uniform distribution of carbon nanotubes in rubber latex.

### FTIR analysis

FTIR technique is often exploited to characterize the formation and occurrence of physical and chemical bonds [22] originated from the fact that these types of bonding can have a key role in infrared spectroscopy. It should be bear in mind that, an esterification reaction between carboxyl groups of XSBR and hydroxyl groups of CNTs to make an ester is quite difficult to proceed in an aqueous media and at room temperature, where as reversed reaction (hydrolysis) may also occur [23].

Presence of –OH groups on the surface of functionalized CNTs and –COOH groups along the polymer chain
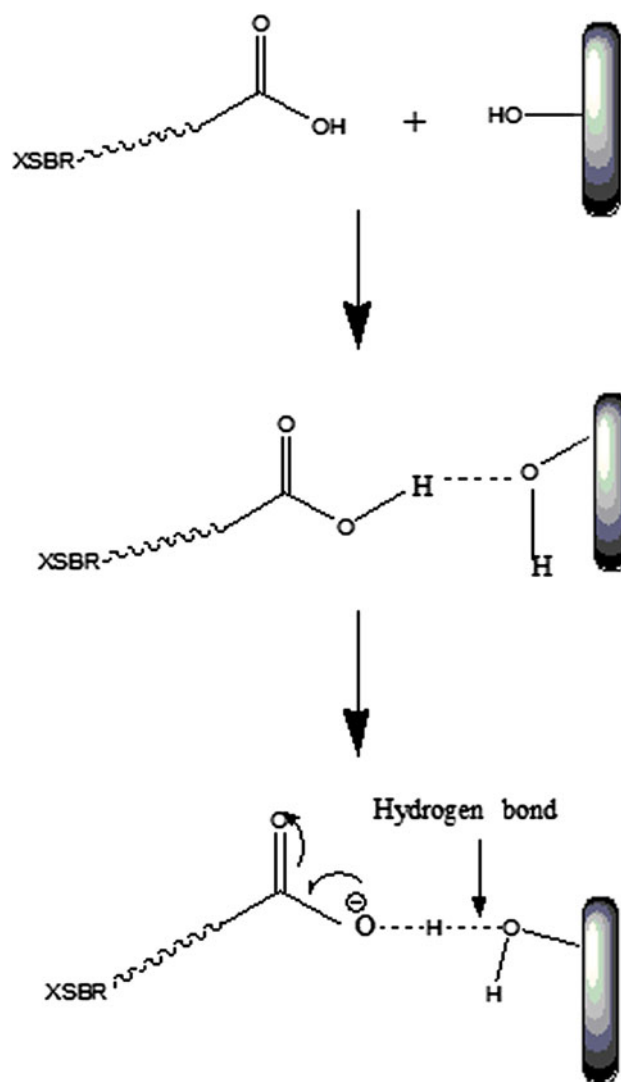


**Fig. 6** Proposed mechanism by which the functionalized CNTs react with carboxylated latex

provides a basis for the physical bonds (particularly H-bonding) between these groups. The high density of H-bonding influences the strength of the bridge made between the polymer chain and nanotube and consequently alters the frequency of bond vibration. Based on the mechanism that we proposed, formation of hydrogen bonding can occur through the hydrogen atom linked to the carboxyl group of XSBR latex and the oxygen of hydroxyl functional group of CNTs as shown in Fig. 6.

In fact, the hydrogen atom of carboxyl group is more acidic than that of hydroxyl, thus, it provides an –OH group on which the density of the electrical charge is more unstable, i.e., quite negative oxygen and very positive hydrogen [24]. The positive hydrogen is now ready to make link with another source of electrons. Here, this source of electrons is provided by the non-bonding electrons of oxygen atom that belong to hydroxyl group

**Scheme 2** Delocalization of electrons in the acetate anion
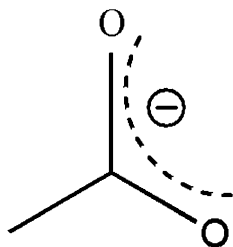
(Fig. 6). As the hydrogen atom is getting involved more in hydrogen bonding, the shared electrons in covalent bond congregate on the oxygen atom linked to C=O, and due to resonance, the electrons of $\pi$ bond of C=O may be resonated between two oxygen atoms of carboxyl group. This process is called delocalization of electrons and can be very clearly seen in the acetate anion (Scheme 2) which is in obvious contradiction to the following structure, as X-ray crystallography shows two oxygen atoms are not distinguishable [24].

Infrared analysis supports this interpretation. ATR spectra of functionalized and non-functionalized CNT composites are exhibited in Fig. 7. Comparing both spectra, all peaks appear at the same wavenumber, however, a short peak is observed at 1,185 cm$^{-1}$ on the spectrum of sample with 2 phr CNTs assigned to the mode of stretching vibration of C–O bond. This peak has been shifted to higher wavenumber of 1,220 cm$^{-1}$ on the ATR spectrum prepared from the sample with the same concentration of CNTs but functionalized.

The frequency up shift is commonly associated with the need for a greater energy of vibration (bending or stretching) of atomic bonds, indicating (in our case) the strengthening of C–O bond for the XSBR/CNTOH nanocomposite. The stronger the bond formed between carbon and oxygen atoms, the shorter is the bond length. An explanation for a shorter bond is the capability of C=O bond of carboxyl group to resonate its $\pi$ electron with
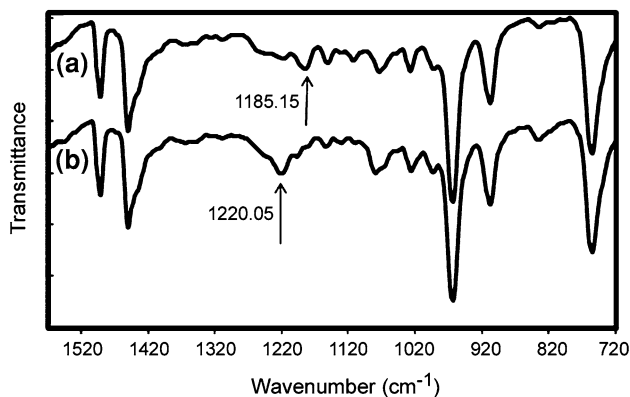
another oxygen atom of this group, C–O, creating a hybrid of single and double bonds between two oxygen atoms, as mentioned above. As a result, a higher energy is required to vibrate oxygen atom in any mode of bending or stretching vibrations, giving rise to relocation of peak at 1,185 cm$^{-1}$ for an up-shift of 35 cm$^{-1}$ to higher energy peak (wavenumber) of 1,220 cm$^{-1}$. It is worth noting that in the case of XSBR/CNTs where the composite consists of non-functionalized nanotube, the same explanation may potentially be given, however, due to the lack of hydroxyl group, which provides a positive hydrogen atom required for the hydrogen bonding, no shift to higher frequency can be observed. No chance of ester formation between functional groups of CNTs and those of XSBR can be considered due to the aqueous medium and low temperature condition, as discussed earlier.

SEM cryosurface analysis

The next part consists of the investigation of cryofractured surface of XSBR/CNTs nanocomposite. The cryogenic fracture was carried out by submerging a thin sample in liquid nitrogen and leaving it there for required time to let the sample reach a temperature below enough its glass transition temperature.

Figure 8a–c show SEM micrographs (at various magnifications) of the fractured surface of nanocomposite prepared by loading 4 phr CNTs (non-functionalized) into the latex. High CNTs content sample was chosen to overcome the difficulties encountered for monitoring and observing two similar substances (CNTs and XSBR are both carbon based materials) thus, SEM pursuing for the state of CNTs dispersion would be easier. As these micrographs indicate, no large agglomerates are visible even on the smaller magnification ones (they are not given here for brevity purposes). It is due to the type of used surface active agent (SDS). The chemical structure of this surfactant is composed of an aliphatic chain (non-polar) of 12 carbon ended by a polar group. While the aliphatic part is principally compatible with CNTs, the polar end makes physical interaction with the carboxyl group of the rubber through non-conjugated electrons of oxygen atoms providing an appropriate distribution and dispersion of CNTs. Role of surfactant on the improvement of CNTs dispersion was comprehensively studied by Vaisman et al. [25] and Rausch et al. [26]. According to the mechanism they proposed the surfactant molecules relocates on the surface of CNTs and encapsulates the CNTs surfaces by their hydrophobic heads while the hydrophilic part reacts physically with carboxyl groups of latex.

The diameter of CNT in the original form and the diameter measured for the CNT in the rubber matrix are in nanometer range with a larger dimension for the former
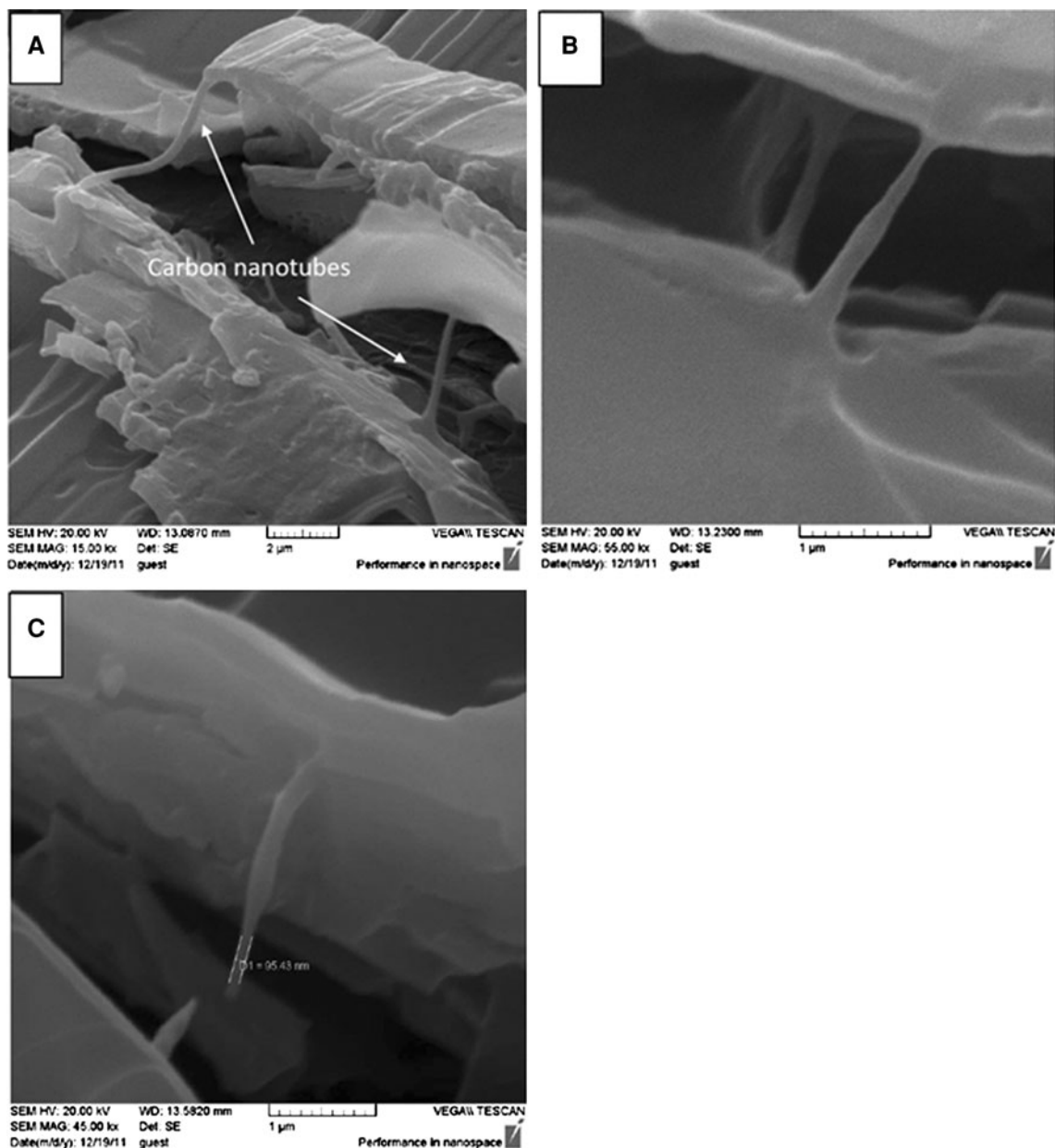


**Fig. 7** FTIR spectra of 2 phr loaded nanocomposites: **a** non-functionalized CNTs and **b** functionalized CNTs

**Fig. 8** SEM micrographs of XSBR nanocomposites containing 4 phr of CNTs

may be attributed to local accumulation of polymer matrix around the MWCNTs. Rubber sheaths were observed around a nanotube or a bundle of few nanotubes when pulled out from the rubber surface during the cryofracture stage. One may discuss and propose about what may consider as an enclosed nanotube, but in fact, it may be a fibrous form of the rubber at fracture surface. This might be correct if the temperature at which the surface made was close to the glass transition temperature of rubber, 0 °C, or the thickness of cryofractured sample was great enough that its core part did not reach temperatures reasonably beneath the $T_g$ of rubber. However, leaving the sample at

temperatures well below its $T_g$ (in liquid nitrogen with a boiling point of $-196$ °C) for quite a long time with its thin thickness, it makes sure of a quite brittle surface fracture free of fibrous parts.

Stress relaxation analysis

Creep and stress relaxation tests are among the experiments applied very commonly to determine the viscoelastic properties of polymers. These tests measure the dimensional stability of a material, since the tests carried out over a long duration, they are of great practical

importance. In a stress relaxation experiment the sample is subjected to a given step deformation and its decay of stress (or modulus) is recorded as a function of time during which the deformation remains constant. The longer the relaxation time, the better can the material retain the stress. This section deals with the stress relaxation of XSBR/CNTs nanocomposites.

A two-step strain method was also used to further investigate the effect of CNTs on the microstructure of resulting nanocomposite. Effects of carbon nanotube concentration on the relaxation behavior of functionalized and non-functionalized CNTs nanocomposites are shown in Figs. 9, 10, respectively. Samples were subjected to a 50 % shear step strain for a duration of 300 s during which modulus relaxes. In a stress relaxation experiment, imposing a step strain leads the macromolecular chains to extend and orient in the direction of applied strain. Once the strain (stress) is employed, the material presents an instantaneous response, however, as time proceeds, a certain portion of molecular chains try to free and relax themselves from the resulting constraint conditions through molecular motions. Commonly, molecular motions may include changes in conformation, slippage of chains with respect to those located in the neighborhood, chain disentanglement and breakup of entanglements, etc [27].

Entanglements, in this respect, play an important role due to both high molecular weight of rubbers and the absence of chemical network. The higher the molecular mobility, the faster is the decay of stress (modulus) and, consequently, the relaxation of polymer. Presence of any foreign material such as fillers, nanotubes, etc. disturbs the relaxation process of polymer by interfering in its chain motions either by making restriction via decreasing the free volume required for the ease of chain mobility or, in contrary, reduction of chain frictions by increasing the free
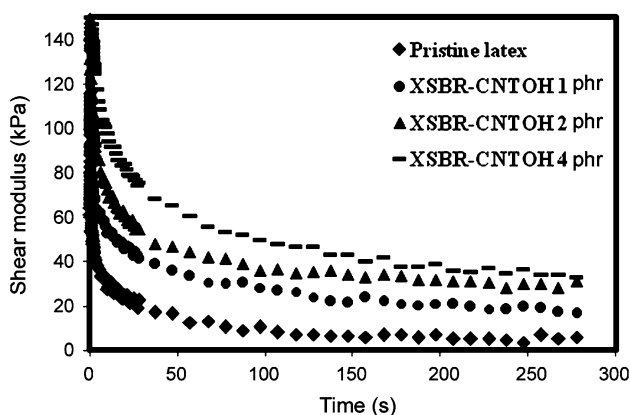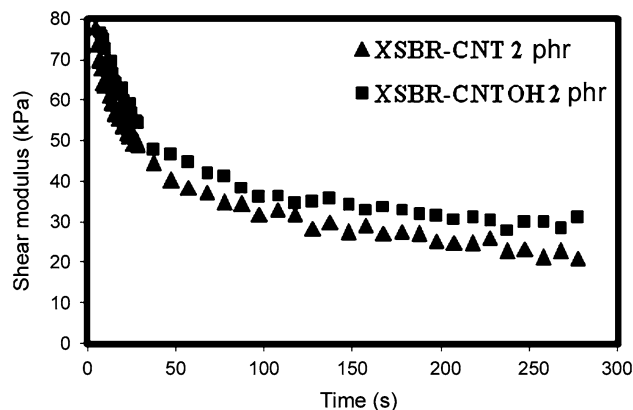


**Fig. 10** Comparison of stress relaxation behavior of functionalized and non-functionalized CNTs nanocomposites

volume and ease of chain mobility. Therefore, a faster or delayed relaxation of polymer from applied stress, to a large extent, depends on the type of additive. An appropriate dispersion of carbon nanotubes in a rubber matrix, however, changes the relaxation behavior of matrix positively, i.e., retards the relaxation process, and improves the viscoelastic properties of polymer.

Functionalized CNTs even cause the relaxation of chains to be further restricted since they are able to make physical bonding (particularly H-bonding) with macromolecular chains in their vicinity through hydroxyl functional group and chain carboxyl groups. The higher the number of bonding between the macromolecules and CNTs functional groups, the stronger would be the polymer/CNTs network. The eventual consequence is increasing in the relaxation modulus of the nanocomposites throughout the relaxation as well as the longer time of relaxation to reach a relaxed modulus ($G_r$) compared with those without CNTs. This behavior is clearly shown in Fig. 10 where the functionalized CNTs compared to the corresponding non-functionalized counterpart have imposed a stronger reinforcing property to the XSBR.

In the second part of this research, the samples are subjected to a programmed stress relaxation experiment. The program includes: (1) employing a 50 % shear step strain and then allowing the sample to relax over a time period of 300 s, (2) stopping the experiment and delaying it for an additional 300 s during which the sample is supposed to approach its original microstructure before starting the second part of the experiment, (3) shear straining the test sample for the second time to the same extent of deformation (50 %) and allowed to relax over another 300 s. The second step shear strain was performed both in the same (+50 %) and in opposite (−50 %) directions with respect to the first strain. This allows the further exploration of the effect of CNTs (functionalized or non-functionalized) on the microstructure and viscoelastic behavior
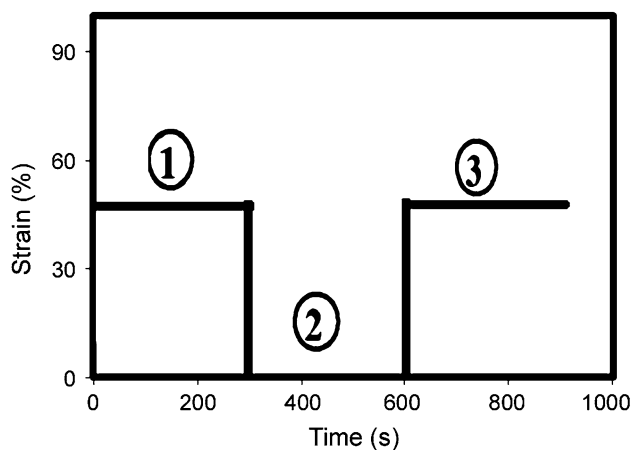


**Fig. 9** Decay of stress as a function of time in stress relaxation experiment for nanocomposites at various concentration of functionalized CNT

Fig. 11 Triple-stage strain imposing: *1* a positive 50 % strain, *2* a 300 s delay free of strain, and *3* a positive 50 % strain



Fig. 12 Triple-stage strain imposing: *1* a positive 50 % strain, *2* a 300 s delay free of strain, and *3* a negative 50 % strain

of nanocomposites of XSBR/CNT. These approaches have been depicted in Figs. 11, 12.

Results of this part of the experiments are demonstrated in Figs. 13, 14, and 16. Figure 13 shows the relaxation behavior of nanocomposite with 2 phr CNT on which a positive–positive stress relaxation is performed. The relaxation behavior of nanocomposite with 2 phr CNT subjected to a positive–negative stress relaxation is represented in Fig. 14.

Figure 16 indicates the difference between relaxation moduli of the sample with 2 phr CNTs when the second step of the experiment (positive and negative) is taken into account. Molecular interpretation of a polymer subjected to stress relaxation experiment has been described in detail else where [27]. However, no information was found when a second experiment (positive or negative), following a short time delay, is applied to the same test sample. When a second stress relaxation experiment is performed on the same test sample, the macromolecules should again be restrained and reoriented in the direction of the applied strain. A positive step strain (at the same direction with respect to first one) results in further orientation of macromolecular chains while a negative one (in opposite direction of first applied strain) leads to a complete new orientation of macromolecular chains. In fact, the previous macromolecular arrangement taken during the first stress relaxation is entirely destroyed.

As it is observed in Figs. 13, 14, for both cases, the resulting relaxation modulus is higher than the value corresponding to the application of first step strain; however, the sample subjected to a negative step strain presents a higher modulus as shown in Fig. 14. As a matter of fact, application of a positive step strain on the test sample means further orientation of the already oriented macromolecules (even though they are relaxed for a limited time duration) resulting in a higher modulus compared to the first step as is
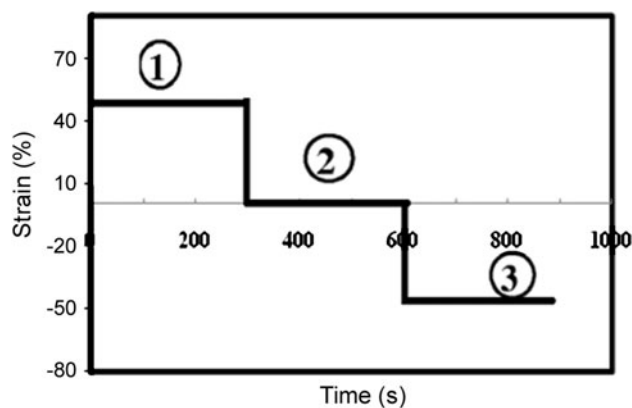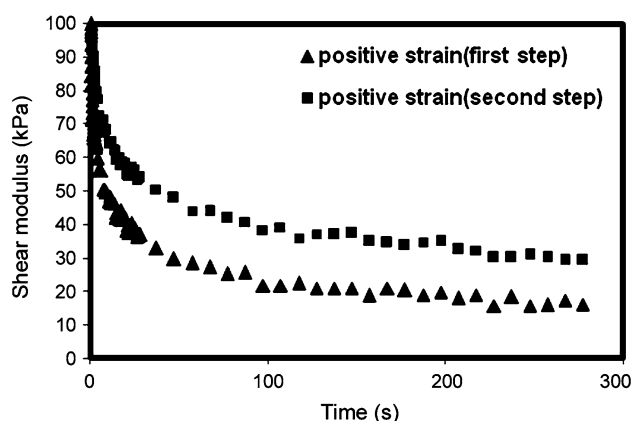


Fig. 13 Comparison of stress relaxation modulus for nanocomposite loaded with 2 phr CNTs subjected to positive–positive two-step strain. A 300 s delay separates two steps
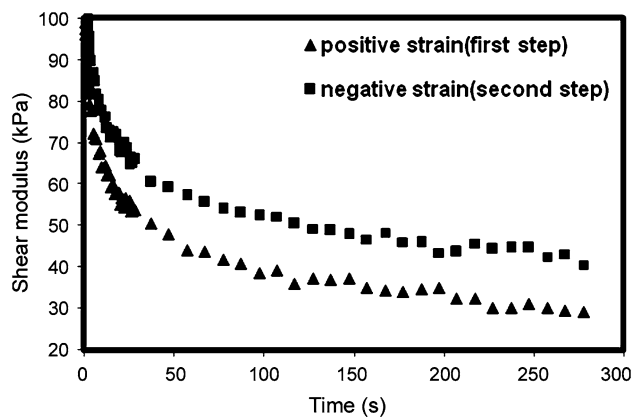


Fig. 14 Comparison of stress relaxation modulus for nanocomposite loaded with 2 phr CNTs subjected to positive–negative two-step strain. A 300 s delay free of strain separates two steps

illustrated in Fig. 15. Nevertheless, the increment is smaller than the case of negative strain, since in the latter case the sample is wholly restrained in opposite direction. This leads
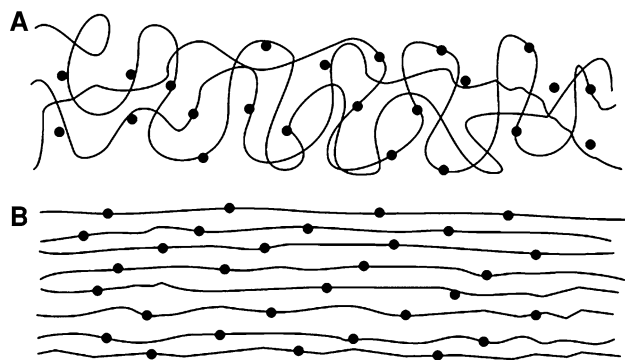
Fig. 15 Schematic view indicating macromolecular chains in coiled (rest) and uncoiled (sheared) states: **a** at rest and **b** sheared [32]
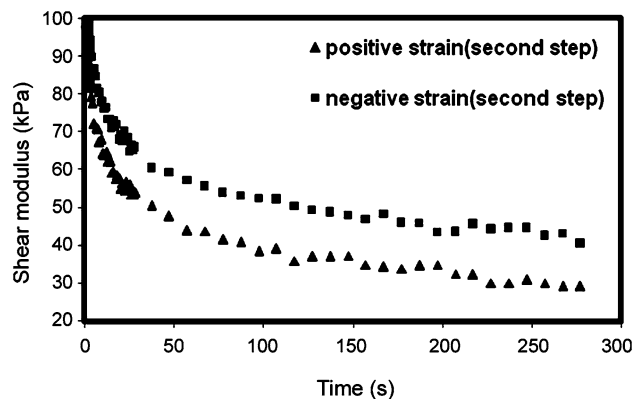


Fig. 16 Comparison between second steps of two-step stress relaxation experiments applied on nanocomposites loaded with 2 phr CNT; positive and negative as second steps

to straining of macromolecules in the reversed path which is associated with various macromolecular resistances including macromolecule displacement, chain slippage and reconformation, chain interlocking through bulky side groups, etc (Fig. 16).

From thermodynamic point of view, chains are forced towards a path over which the entropy further decreases and the more energy consumes resulting in a higher modulus. The addition of CNTs to XSBR, although makes no change in overall trend of nanocomposites behavior, however, increases the difference between the first and second step relaxations. The higher the amount of CNTs in nanocomposite, the larger is the difference between the relaxation moduli of the first and second steps irrelevant of the direction of straining. Presence of CNTs with functional groups intensifies this behavior, and the observed differences between relaxation moduli of first and second steps increases further.

Relaxation process modeling

The relaxation modulus can be regarded as a function of time and temperature, i.e., $G = G(t, T)$. The stress developed as a result of imposed strain may also be given as follows:

$$\sigma = G(t, T) \cdot \gamma_0 \tag{2}$$

where, $\sigma$ is the shear stress and $\gamma_0$ is the applied constant shear strain. At a constant temperature:

$$\sigma = G_{iso}(t) \cdot \gamma_0 \tag{3}$$

where, $G_{iso}(t)$ is the time dependent relaxation modulus at constant temperature, henceforth, represented as $G(t)$. Mathematical analysis of the creep and relaxation phenomena is frequently carried out using mechanical elements of spring and dashpot, particularly generalized Maxwell or Voigt models. Using a generalized Maxwell model with infinite number of elements, the time dependent modulus, $G(t)$, is given as follows [27]:

$$G(t) = G_r + \int_{-\infty}^{+\infty} H(\tau) \cdot e^{-t/\tau} d \ln \tau \tag{4}$$

where, $H(\tau)d \ln \tau$ is the contribution to rigidity associated with relaxation times between $\ln \tau$ and $\ln \tau + d \ln \tau$. $G_r$ is the modulus at infinite $\tau$. The longer the relaxation time, the more capable is the material to retain the initial modulus. A generalized Maxwell model including a large number of Maxwell elements in parallel was proposed to predict the stress relaxation of real polymers. Each element has a specified relaxation time of $\tau_i$. Supposing a generalized Maxwell model with $N$ elements, the corresponding equation for the stress relaxation is given as:

$$G(t) = \sum_{i=1}^{N} G_i \cdot e^{-t/\tau i} \tag{5}$$

Prony series which is an array of Maxwell elements in parallel with an extra spring, $k_e$, also in parallel, is one of the best approaches predicting the time dependent behavior of elastomers and other viscoelastic materials. Each term of the Prony series is represented by one Maxwell element. The corresponding equation is described as follows:

$$G(t) = \sum_{i=1}^{N} g_i (1 - e^{-t/\tau_i}) \tag{6}$$

where, $g_i$ and $\tau_i$ are the material parameters, and $g_R(t)$ is the relaxation modulus expressed as a dimensionless normalized relaxation modulus, i.e., $g_R(t) = G(t)/G_o$ where $G_0$ is the shear modulus when $t \rightarrow 0$.

Nowadays computers have facilitated the use of complicated models for the prediction of rheological and mechanical properties of polymers. Mottahedi et al. [28] used ANSYS software to numerically analyze the stress relaxation experiment based on the Prony series. Chen
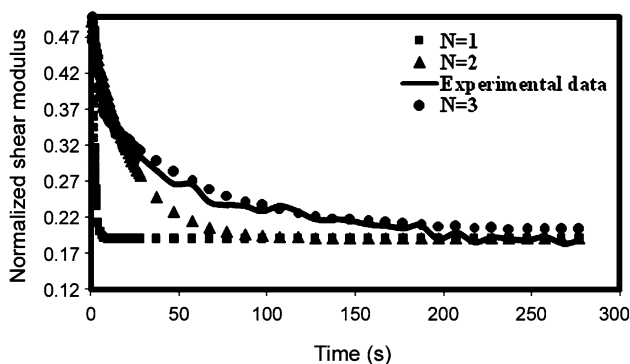
**Fig. 17** Model prediction of stress relaxation experiment for a second negative strain for nanocomposite loaded with 2 phr CNT using Prony series at various $N$ values
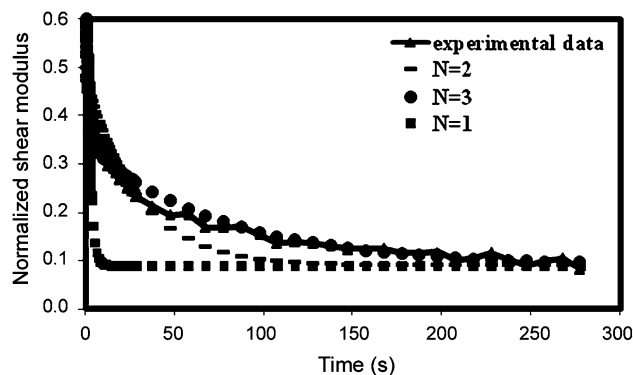


**Fig. 18** Model prediction of simple stress relaxation experiment (one-step) for nanocomposite loaded with 2 phr CNT using Prony series at various $N$ values

[29], Ghorieshy [30] and Ha [31] applied ABAQUS software to obtain the Prony series parameter for different purposes. In the present study ABAQUS/Standard software [30] was applied to acquire the fitting parameters of Prony series. As shown in Fig. 17 the Prony series with $N = 1$ and 2 cannot suitably predict the experimental results, however, the prediction is rather better when $N = 3$ is chosen. The corresponding parameters of $g_i$ and $\tau_i$ for various $N$ have been provided in Table 1.

This procedure was also applied for the prediction of stress relaxation behavior of the samples subjected to the second step strain and the results have been demonstrated in Fig. 18 and Table 2. One may state that obtaining Prony series parameters does not individually well worth; however, this might be a misconception. Considering that these parameters can pave the way to obtain constitutive equations describing viscoelastic properties of polymer will disclose the value of aforesaid simulation. For instance, the following equations, used to describe the frequency dependence of elastic and loss moduli, are based on the Prony series parameters.

$$G'(\omega) = G_0 \left[ 1 - \sum_{i=1}^{N} g_i^p \right] + G_0 \sum_{i=1}^{N} \frac{g_i^p \tau_i^2 \omega}{1 + \tau_i^2 \omega} \quad (7)$$

$$G''(\omega) = G_0 \sum_{i=1}^{N} \frac{g_i^p \tau_i \omega}{1 + \tau_i^2 \omega^2} \quad (8)$$

In this work, dynamic mechanical experiments are predicted using these equations and Prony series parameters.

**Table 1** Prony series parameters obtained for XSBR/CNTs nanocomposite loaded with 1 phr, at first step of a two-step experiment, $N = 3$

| | | | |
|---|---|---|---|
| $g_i$ | 0.3817 | 0.2848 | 0.2515 |
| $\tau_i$ | 0.1367 | 2.459 | 75.88 |

**Table 2** Prony series parameters obtained for XSBR/CNTs nanocomposite loaded with 1 phr at second step of a two-step experiment, $N = 3$

| | | | |
|---|---|---|---|
| $g_i$ | 0.3757 | 0.2472 | 0.1891 |
| $\tau_i$ | 0.1435 | 2.204 | 60.19 |

## Conclusion

XSBR/MWCNTs nanocomposites prepared in a ball mill were studied. This method of preparation in controlled conditions can create an excellent dispersion and break the CNTs bundles. The results obtained indicate an enhancement in both rheological and viscoelastic properties, observed for both functional and non-functional CNTs. Presence of hydroxyl functional group on the surface of CNTs through making interaction with polymer chains not only affected on the improving of rubber properties further but also aided more uniform distribution and dispersion of CNTs. ATR analysis confirmed the presence of physical interaction of H-bonding type. SEM images exhibited a good dispersion of nanotubes in the rubber matrix. Stress relaxation experiments were applied as a complementary and confirming approach to investigate the microstructure of CNTs nanocomposites. The results obtained indicated an increase in the relaxation modulus of polymers in the presence of CNTs particularly functionalized one. Imposing a second step strain to polymer chains, either positive or negative, resulted in higher relaxation modulus compared to the first step strain, however, higher values obtained for the modulus where a negative second step strain was applied. Prony series successfully predicted the stress relaxation behavior of XSBR/CNTs nanocomposites.

Iran Polymer and Petrochemical Institute     Springer

# References

1. Huang YY, Ahir SV, Terentjev EM (2006) Dispersion rheology of carbon nanotubes in a polymer matrix. Phys Rev B 73:1–9

2. Ivanov E, Kotsilkova R, Krusteva E, Logakis E, Kyritsis A, Pissis P, Silvestre C, Duraccio D, Pezzuto M (2011) Effects of processing conditions on rheological, thermal, and electrical properties of multiwalled carbon nanotube/epoxy resin composites. J Polym Sci, Part B: Polym Phys 49:431–442

3. Via MD, Morrison FA, King JA, Caspary JA, Mills OP, Bogucki GR (2011) Comparison of rheological properties of carbon nanotube/polycarbonate and carbon black/polycarbonate composites. J Appl Polym Sci 121:1040–1051

4. Yan XL, Gong Z, Gong J, Gao S, Zhang Z, Wang B (2012) Investigation of the rheological and conductive properties of multi-walled carbon nanotube/polycarbonate composites by positron annihilation techniques. Carbon 50:2899–2907

5. Cheng HKF, Pan Y, Sahoo NG, Chong K, Li L, Chan SH, Zhao J (2012) Improvement in properties of multiwalled carbon nanotube/polypropylene nanocomposites through homogeneous dispersion with the aid of surfactants. J Appl Polym Sci 124: 1117–1127

6. Kim M, Mun SC, Lee CS, Lee MH, Son Y, Park OO (2011) Electrical and rheological properties of polyamide 6, 6/$\gamma$-ray irradiated multi-walled carbon nanotube composites. Carbon 49:4024–4030

7. Rahmatpour A, Kaffashi B, Maghami S (2011) Preparation and rheological properties of functionalized multiwalled carbon nanotube/waterborne polyurethane nanocomposites. J Macromol Sci Part B Polym Phys 50:1834–1846

8. Pötschke P, Fornes TD, Paul DR (2002) Rheological behavior of multiwalled carbon nanotube/polycarbonate composites. Polymer 43:3247–3255

9. Du M, Guo B, Lei Y, Liu M, Jia D (2008) Carboxylated butadiene–styrene rubber/halloysite nanotube nanocomposites: interfacial interaction and performance. Polymer 49:4871–4876

10. Peterson SC, Jong L (2008) Effect of wheat flour pre-cooking on the composite modulus of wheat flour and carboxylated styrene–butadiene latex. Compos Part A Appl S 39:1909–1914

11. Pietrasik J, Gaca M, Zaborski M, Okrasa L, Boiteux G, Gain O (2009) Studies of molecular dynamics of carboxylated acrylonitrile-butadiene rubber composites containing in situ synthesized silica particles. Eur Polym J 45:3317–3325

12. Jubete E, Liauw CM, Allen NS (2007) Water uptake and tensile properties of carboxylated styrene butadiene rubber based water born paints: models for water uptake prediction. Prog Org Coat 59:126–133

13. Stephen R, Alex R, Cherian T, Varghese S, Joseph K, Thomas S (2006) Rheological behavior of nanocomposites of natural rubber and carboxylated styrene butadiene rubber latices and their blends. J Appl Polym Sci 101:2355–2362

14. Blackley DC (1997) Polymer latices, chap 1. Springer, UK, pp 15–17

15. Hirscher M, Becher M, Haluska M, Von Zeppelin F, Chen X, Dettlaff-Weglikowska U, Roth S (2003) Are carbon nanostructures an efficient hydrogen storage medium? J Alloys Compd 356:433–437

16. Awasthi K, Kamalakaran R, Singh AK, Srivastava ON (2002) Ball milled carbon and hydrogen storage. Int J Hydrogen Energy 27:425–432

17. Li YB, Liang J, Wei BQ, Liang J, Yu Q, Wu DH (1999) Transformation of carbon nanotubes to namnoparticle by ball milling process. Carbon 37:493–497

18. Ma PC, Wang SQ, Kim J-K, Tang BZ (2009) In situ amino functionalization of carbon nanotubes using ball milling. J Nanosci Nanothecno 9:749–753

19. Macosko WC (1994) Rheology principles, measurements and applications, Chap 4. USA, pp 134–174

20. Gent AN (2001) Engineering with rubber how to design rubber components, chap 4. Hanser, USA, pp 74–78

21. Sperling LH (2006) Introduction to physical polymer science, chap 5. Wiley, USA, pp 217–218

22. Stuart B (2004) Infrared spectroscopy fundamentals and applications, chap 3. Wiley, UK, pp 49–53

23. Otera J, Nishikido J (2010) Esterification methods, reactions, and applications, chap 1. Wiley, Germany, pp 11–13

24. Sykes P (1985) A guidebook to mechanism in organic chemistry, chap 1. Wiley, USA, pp 19–21

25. Vaisman L, Wagner HD, Marom G (2006) The role of surfactants in dispersion of carbon nanotubes. Adv Colloid Interface Sci 128–130:37–46

26. Rausch J, Zhuang R-C, Mäder E (2010) Surfactant assisted processing of carbon nanotube/polypropylene composites: impact of surfactants on the matrix polymer. J Appl Polym Sci 117:2583–2590

27. Ferry JD (1980) Viscoelastic properties of polymers, chap 4. Wiley, New York, pp 47–69

28. Mottahedi M, Dadalau A, Hafla A, Verl A (2011) Integrated systems, design and technology, chap 8, 1st edn. Springer, New York, pp 79–91

29. Chen T (2000) Determining a prony series for a viscoelastic material from time strain data. NASA/TM-210123 ARL-TR-2206

30. Ghoreishy MHR (2012) Determination of the parameters of the Prony series in hyper-viscoelastic material models using the finite element method. Mater Design 35:791–797

31. Ha J (2008) Carbon black filler reinforcement of elastomers. A thesis submitted to the University of London

32. Chhabra RP, Richardson JF (2008) Non newtonian flow and applied rheology, chap 1. Butterworth-Heinemann, UK, pp 38–41